Characterization and Micro-assembly of Electrostatic Actuators for 3-DOF Micromanipulators in Laser Phonomicrosurgery

Eakkachai Pengwang
Institute of Field Robotics
King Mongkut's University of Technology Thonburi
126 Pracha-Utid Road, Bangmod, Thungkru, Bangkok
10140 THAILAND
eakkachai@fibo.kmutt.ac.th

Kanty Rabenorosoa, Micky Rakotondrabe, Nicolas Andreff
FEMTO-ST Institute
UMR CNRS 6174-UFC/ENSMM/UTBM
Automatic Control and Micro-Mechatronic Systems Department, Besançon, 25000 FRANCE

***Abstract*— This paper presents a design of electrostatic actuators for 3-DOF micromanipulators in robot-assisted laser phonomicrosurgery. By integrating three sets of electrostatic actuators in a vertical configuration, scanning micro-mirror can be used as a manipulator for laser source. Key enable technology for these miniaturized actuators is microfabrication processes for microelectromechanical systems (MEMS) because the processes can create submicron features with high precision, mass productive, and low cost. Based on precise micromachined electrostatic actuators, the platform is assembled using micro assembly approach. With sizes less than 5 mm x 5 mm x 5 mm, the proposed design has three degree-of-freedom: two rotational motions around the in-plane axis and one out-of-plane translational motion. Static and dynamic analysis of the device is simulated by Finite Element Analysis (FEA) and compared to theoretical calculations. This system preserves outstanding characteristics of electrostatic actuators for fast response and low power consumption. By micro-assembly of the scanning micro-mirror, the endoscopic systems can be created with a high range of motion and high scanning speed. The target applications of this system include laryngeal microsurgery, optical coherence tomography (OCT), and minimally invasive surgeries (MIS).**

Keywords— Electrostatic actuators; Micromanipulators; Micro-assembly; Micromirrors; Phonomicrosurgery; laryngeal surgery

Research supported by MicroRALP project (European Framework 7th) and the FEMTO-ST Institute, UMR CNRS 6174-UFC/ENSMM/UTBM, Automatic Control and Micro-Mechatronic Systems Department, Besançon, 25000 FRANCE.

Eakkachai Pengwang is with the FEMTO-ST Institute UMR CNRS 6174-UFC/ENSMM/UTBM, Automatic Control and Micro-Mechatronic Systems Department (AS2M), France and now working at the Institute of Field Robotics, King Mongkut's University of Technology Thonburi, Thailand (corresponding author to provide phone: 66-2470-9715; fax66-2470-9714; e-mail: eakkachai@fibo.kmutt.ac.th).

Kanty Rabenorosoa, Micky Rakotondrabe, and Nicolas Andreff are with the FEMTO-ST Institute UMR CNRS 6174-UFC/ENSMM/UTBM, Automatic Control and Micro-Mechatronic Systems Department (AS2M), Besançon, 25000 FRANCE.

I. INTRODUCTION

There are many classifications of actuating micro-mirror devices. One method to distinguish these devices is by the numbers of allowable motions of the mirror and type of the motion. Since different applications require different manipulations, specific design considerations are studied for better manipulators. For laryngeal microsurgery, a suitable micro robot should consist of three crucial degrees-of-freedom; that are two rotational motions around the in-plane axis and one out-of-plane translational motion. The translation along the in-plane motion and the in-plane rotation are not critical since these parameters will not change the directions and orientation of the laser sources. Sometimes, this type of micro robots is referred as a tip-tilt-piston micro scanning mirror. The target size of the micro robots for phonomicrosurgery should be less than 5 millimeters for a footprint. The total volume should be less than 125 cubic millimeters. An implementation of micro-mirror for laser phonomicrosurgery is shown in Fig. 1.

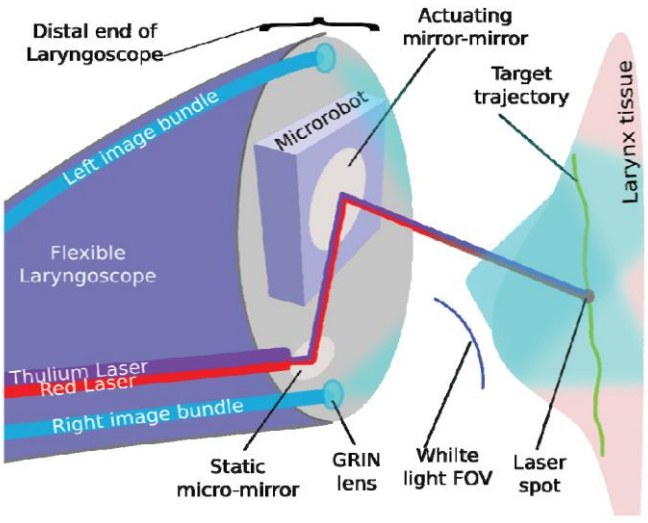

Figure 1: Micro-mirror scheme for robot-assisted laser phonomicrosurgery.

In the past decades, several forms of micro-mirrors have been investigated for optical applications and laser phonomicrosurgery, for example, electrostatic actuators [1-8], electrothermal actuators [9-12], piezoelectric actuators [13-14], electromagnetic actuators [15], acoustic actuators, pneumatics actuators, and shape memory alloys [16]. Electrostatic actuators are implemented in many applications such as accelerometers, scanning mirrors, photonics, televisions, and projectors. The limitation of electrostatic actuators can be a pull-in voltage and high driving voltage on the order of 100 V. For medical application, micro scanning mirror with electrostatic actuators are also investigated widely for optical coherence tomography (OCT) because they are fast response, consume low power, and yield large scanning angle. In this paper, design and analysis of micro robots are investigated with suitable actuators and mechanism. Our design will focus on micro-assembly with three sets of linear electrostatic comb drives to generate a tip-tilt-piston micro-mirror.

In this paper, design of 3-DOF electrostatic micro-mirrors for laser phonomicrosurgery is explained in Section II. The investigation for actuating micro-mirrors from both theoretical calculation and finite element modeling are given in section III, and IV, respectively. In section V, microfabrication processes of electrostatic actuators are explained in detail. Next, the experimental results are compared to the theoretical and simulation in Section VI. Last, the micro-assembly of electrostatic micro-actuators is presented in Section VII. Section VIII concludes the paper.

II. DESIGNS

In this paper, electrostatic actuators are chosen and combined to create a motion for scanning micro-mirrors. An objective is to investigate the performance of the linear comb drive and process of micro-assembly of electrostatic actuators with a planar micro-mirror. Schematic of micro-mirror with three sets of electrostatic actuators are presented in Fig. 2. The device is made of silicon-on-insulator (SOI) substrate structured by microfabrication techniques. The processes of micro-electromechanical systems (MEMS) are suitable for this design because they can create submicron features with high precision, mass productive, and low cost.

One of the main challenges for using three electrostatic actuators is to assembly them in a precise manner. Regards to positions and orientations of the actuator, a new scheme to assembly linear electrostatic actuators by using V-groove marker and spring-lock mechanism are presented. CAD models of micro-actuators with assembly components are presented in Fig. 3. After the fabrication of the micro-actuators, the electrostatic actuators are assembled to the mirror with small complaints as shown in the assembly box in Fig. 4.

The total dimension of the micro-assembly is 6 mm x 4 mm x 4 mm for the assembly box, while the size of micro-actuators is 4.5 mm x 2 mm x 0.3 mm. This method is designed for micro-assembly process, not only for linear electrostatic actuator, but it can be implemented for integrations of several transducers, sensor, and microsystems that require a precision assembly. With the precise locations and orientations of the

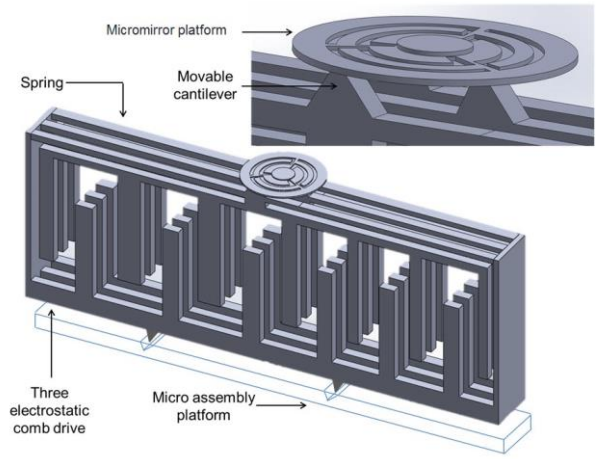

Figure 2. Schematic of micro-manipulator design for robot-assisted laser phonomicrosurgery with electrostatic micro-actuators.

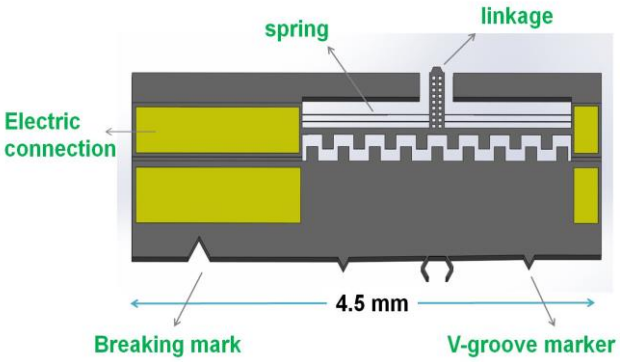

Figure 3. Micro-assembly part with markers and breaking parts

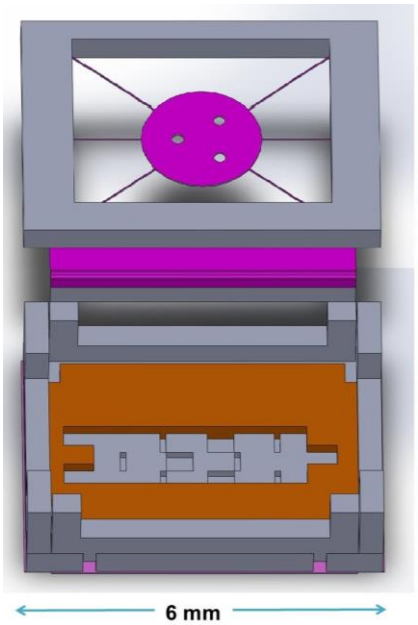

Figure 4. Micro-assembly block with markets and slots

actuators, this type of micro-manipulator can be an alternative method for microdevices and microsystems as well.

III. THEORETICAL CALCULATION

The principle of electrostatic actuator is the static charge phenomena in each pair of adjacent comb finger. The actuator can generate electrostatic force by the change of capacitance. In order to stabilize the comb-drive, the mechanical stiffness of the comb drive is connected to the spring and the anchor.

The governing equations of motion for general comb-drive actuators involve parameters on gap between electrodes (d), thickness of comb finger (t), supplied voltage (V), and spring constant for beam suspensions (k_{eff}). The deflection (δ_{comb}) of comb-drive actuators connected to beam suspensions is given by Equation 1.

$$\delta_{comb} = \frac{F_{comb}}{k_{eff}} = n \cdot \frac{\varepsilon \cdot t \cdot V^2}{d} \cdot \frac{L^3}{4 \cdot E_{spring} \cdot h \cdot b^3} \quad (1)$$

where F_{comb} is the electrostatic force due to comb actuator, n is the number of pairs of comb fingers, ε is permittivity of the media, L is the length of the beam suspension, E is the Young's modulus of the material, b is the width of the spring, and h is the height of the spring. It is also noted that the height of the device does not influence the defection if the thickness of the beam suspension and comb fingers are the same. In this study, two main designs are proposed for the beam suspension; single beam with four legs (Design A), and folded beam with two anchors and two legs for each side (Design B). The comparison between each design will be examined and characterized in the following sections.

For 100 pairs of electrostatic actuators with a thickness of 15 μm and the gap of 6 μm, the electrostatic force at 100 V is 20.6 μN. For design A (four single spring suspension), the stiffness of systems is about 0.97 N/m. When all three actuators are supplied with the same voltage, the piston motion of electrostatic comb-drive is 21.3 μm. With the same actuating force, design B can generate about 28.68 μm. For design B (four double-folded spring suspension), the stiffness of systems is about 0.72 N/m. With a design distance of 800 μm between each pin on the mirror platform on the top, the optical scanning angle of the mirror can be 4.1 degrees.

IV. SIMULATIONS

Simulation results by COMSOL® Finite Element Analysis (FEA) software show that the linear electrostatic in design A can move up to 11.2 μm when it is actuated at 100 V. From calculation, the maximum optical scanning angle is about 1.6 degrees with a piston motion of 11.2 μm. The simulation result for total displacement is demonstrated for one set of electrostatic actuators at 100 V as shown in Fig. 5. Dynamical analysis can be also simulated by COMSOL® software. The designed structure is tested for six natural frequencies. The first natural frequency is at 1017.9 Hz.

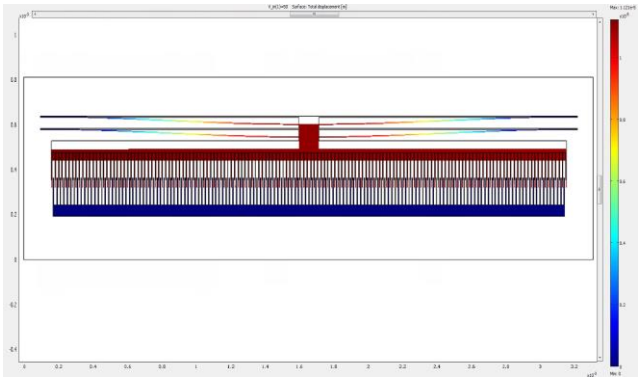

Figure 5. COMSOL® simulation result for single-beam suspension (Design A) shows the displacement of 12 μm.

V. MICROFABRICATION PROCESS

Based on precise micromachined electrostatic actuators, the platform is assembled using micro assembly approach. With sizes less than 5 mm x 5 mm x 5 mm, the proposed design has three degree-of-freedom: two rotational motions around the in-plane axis and one out-of-plane translational motion. The microfabrication process of the linear electrostatic actuator and mirror is shown in Fig. 6. SOI wafer with device layer of 15 μm on a 500-μm-thick handle layer is patterned for electrical pads and structure for electrostatic comb drive. Chrome and gold is deposited and patterned for electrical pad by photolithography and wet etchant (Fig. 6a). Next, the mask for structure is patterned by photoresist and deep reactive-ion-etching (DRIE) on the device layer (Fig. 6b). The high-aspect-ratio structure is created by a deep-reactive-ion-etching (DRIE) process. The alignment mark on the front side is then used to align the backside etching mask on the handling layer (Fig. 6c). The process of reactive-ion-etching is used for etching the backside (Fig. 6d). Then, the wafer is immersed in vapor hydrofluoric acid to remove the oxide layer (Fig. 6e). Last, all of phororesist mask is removed to complete the electrostatic actuators with cantilever (Fig. 6f). The electrostatic actuators are then separated from the entire wafer and ready to assembly. With the same processes, the planar micro-mirror is also fabricated with thin-film gold in the first step to improve reflectivity for laser source.

From the SEM images, the fabricated devices are smaller than the design values. The spring suspensions are 7 μm in width (the design value is 8.5 μm). The length of the springs in design A is 1500 μm. The lengths of the springs in design B (double-folded beam) are 1500 μm and 1050 μm. The comb fingers are 120 μm in length and 9 μm in width (the design value is 12 μm). The distance between adjacent comb fingers are with 6 μm (the design value is 3 μm). The thickness of the electrostatic actuators is 14.2 μm.

The cantilever in the center part is then used to assemble to the micro mirror with certain distance apart from each other. The precise micro assembly is enabled by alignment marks of V-shape and sideway blocks to strengthen the device at the position. Next, micro mirror is placed and glued to the top of

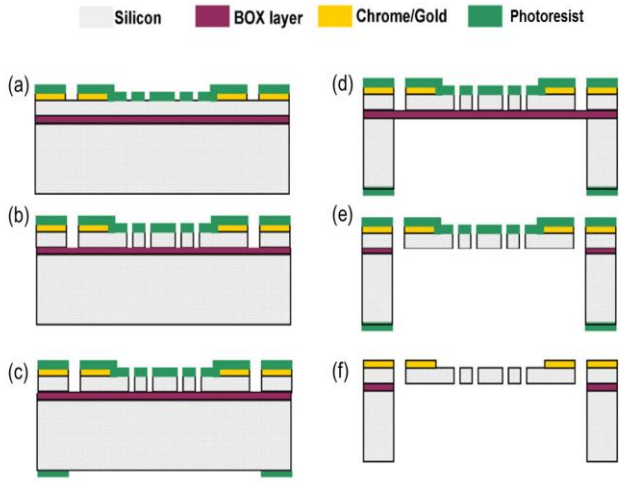

Figure 6. Microfabrication process of electrostatic actuators and mirror for phonomicrosurgery

the three cantilevers to complete the first generation of the device. The fabricated electrostatic actuators are presented in Fig. 7 with breaking mark and V-groove marker for micro-assembly purpose. In the future work, the micro-actuator designs with two rows of electrostatic actuators will be studied. In Fig. 8, alternative for design B with the two rows of electrostatic is shown to enhance the performance of the micromanipulators in laser microsurgery. From the calculation, the required voltage for reaching the same displacement can be reduced by 30% from that value for one row of electrostatic actuators.

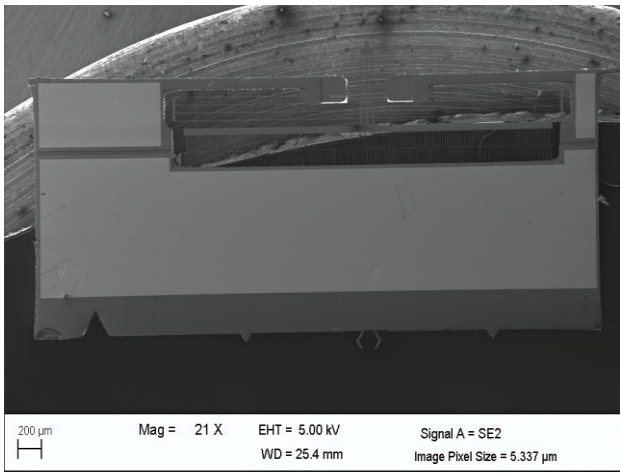

Figure 7. Micro-actuator with electrostatic comb-drives with breaking part, V-groove markers, and flexure springs for assembly (design B).

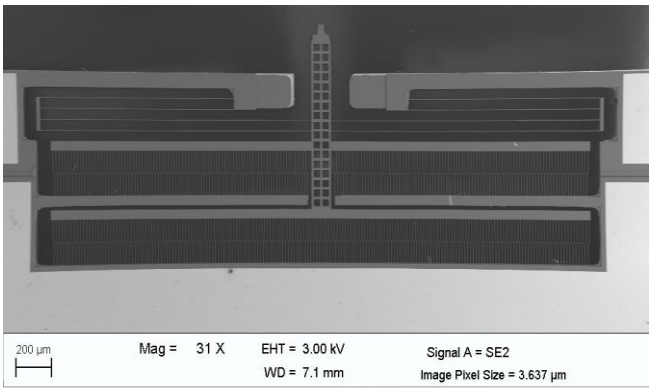

Figure 8. Alternative design for micro-actuator with two set of electrostatic comb-drives

VI. TESTING RESULTS

The static responses of a single electrostatic comb-drive are tested with different voltages. The set-up scheme for testing and measuring displacement of electrostatic comb is shown in Fig. 9. After recording of microscopic images, movements are calibrated and measured using ImageJ® software. The results of static displacement of one actuators with double-folded-beam suspensions are presented in Fig. 10.

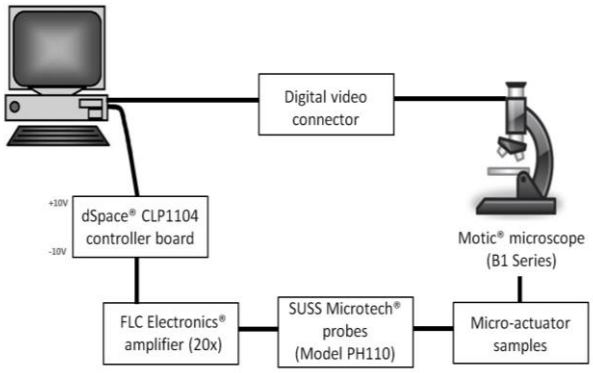

Figure 9. Schematic of the apparatus used for measuring static displacement of electrostatic micro-actuators

The performances of single-beam suspension and double-folded beam suspension are compared. It is observed that the single beam suspension provides smaller displacement than the double-beam suspension. The experimental results show a displacement of 53 µm with 80 V. This value of supplied voltage is lower than 100 V that make it suitable for biomedical systems as well. The comparisons between the performances of electrostatic actuators, the theoretical calculation (in Section III), and the COMSOL simulation (in Section IV) are shown in Fig. 10. Moreover, the testing is repeated to confirm the performance for different samples as shown in Fig. 11.

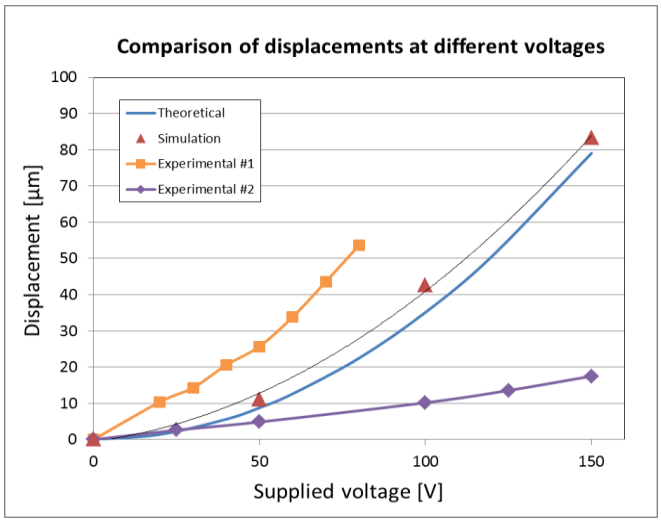

Figure 10. Comparison of performances between theoretical results, simulation results, and experimental results (static mode). Experimental result #1 (orange dots) is a device with double-folded-beam suspensions and experimental result #2 (purple dots) is a device with single-beam suspension.

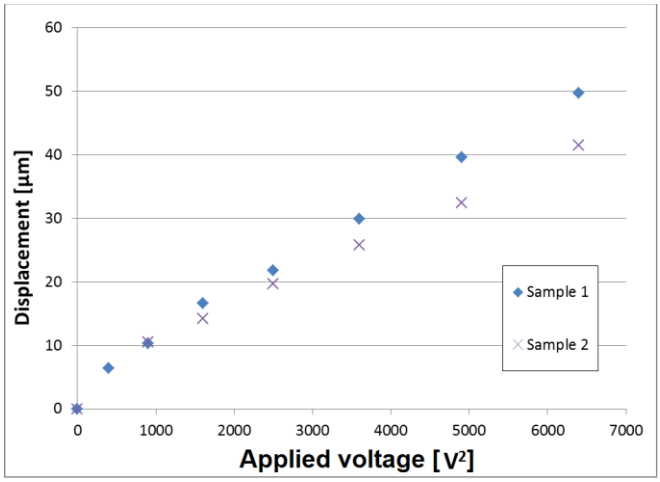

Figure 11. Two samples are tested for the performances at different supplied voltage (a device with double-folded-beam suspension).

The electrostatic actuator are examined and characterized by the Polytec® Micro System Analyzer (MSA-500 Model, Chatillon, France) and the Planar Motion Analyzer software (PMA Version 2.6). The displacement of the single electrostatic actuator at different frequency is shown in Fig. 12. The electrostatic samples (both design A and B) are tested for the resonant frequency that will result to the maximum displacement. From the analysis, the first natural frequency of the electrostatic actuator with design A and design B is about 2380 and 840 Hz respectively. The maximum displacement at resonant frequency is about 19 µm and 33 µm for design A and design B respectively. These values are slightly different from the calculation and simulation. This is possibly due to the spring suspension which is smaller than the design values and

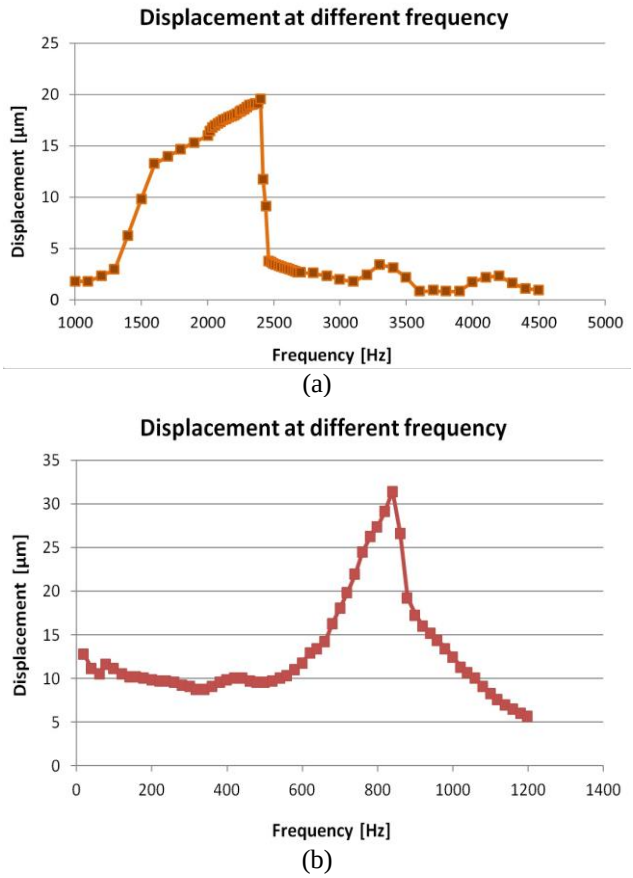

Figure 12. Dynamics analysis for electrostatic actuators at different frequencies (a) a device with single-beam suspensions (b) a device with double-folded-beam suspensions.

the gap between the comb drives which are larger than the expected in the design. However, the detailed analysis on the performance of electrostatic comb-drives will be investigated in the future work.

VII. MICRO-ASSEMBLY OF MIRROR PLATFORM

The design of micro-mirror with three electrostatic actuators are verified and examined for performance. By micro-assembly of three linear electrostatic actuators, the platform can manipulate for three degree-of-freedoms (tip-tilt-piston). The mechanisms of V-groove and silicon spring lock are implemented to ensure that the device is in the precise location and orientation. The epoxy glue is used to strengthen the position of the actuators to the base substrate. The preliminary samples are tested for a quick prototype and it is shown in Fig. 13. According to the results, the assembly processes are successful with the planar mirror on the top of the electrostatic actuators. With the linkages between the cantilevers and the planar mirror, this micromanipulator will be tested and characterized for the performances. The expected result will be a piston motion of 50 µm and the rotation angles of 3.8 degrees.

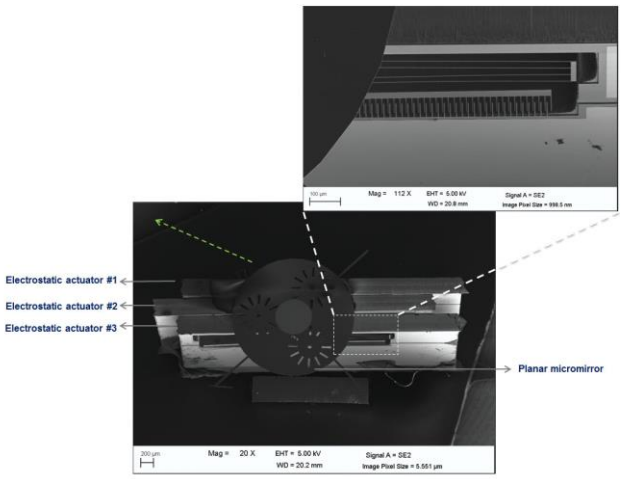

Figure 13. Micro-assembly of three electrostatic comb-drives with a planar micro-mirror

VIII. CONCLUSION

This paper presented a design for 3-DOF (tip-tilt-piston) micro-mirror for phonomicrosurgery applications with electrostatic actuators. The testing results on the two designs (single-beam and double-folded-beam suspensions) are examined. The maximum displacement of 53 µm is achieved with double-folded-beam suspensions at 80 V of supplied voltage. The dynamic responses of these electrostatic actuators are 2380 and 840 Hz with a displacement at resonant frequency is about 19 µm and 33 µm, for single-beam and double-folded-beam suspensions, respectively. Moreover, the microfabricated devices are assembled using a micro-assembly approach with marker and assembly block to place three electrostatic comb-drives in the precise position. In this paper, the preliminary tests of micro-assembly are demonstrated. MEMS-based micro-mirror designs have been enhanced for biomedical apparatus that require high speed, low power consumption, and high reliability.

ACKNOWLEDGMENT

The authors gratefully acknowledge the support by the Micro-Technologies and Systems for Robot-Assisted Laser Phonomicrosurgery (µRALP project) that is a part of the European Union Seventh Framework program FP7/2007-2013 – Challenge 2 – Cognitive systems and robotics. This work has been partially supported by the Labex ACTION project (contract "ANR-11-LABX-01-01", the French RENATECH network, and its FEMTO-ST technological facility.

REFERENCES

[1] K. Laszczyk, S. Bargiel, C. Gorecki, J.J. Krezel, P. Dziuban, M. Kujawinska, M. Kujawinskab, D. Callet, and S. Frank. "A two directional electrostatic comb-drive XY micro-stage for MOEMS applications," *Sensors Actuators A*, vol. 163, pp. 255-265, July 2010.

[2] D. Mukhopadhyay, J. Dong, E. Pengwang, and P. Ferreira. "A SOI-MEMS based 3-DOF planar parallel-kinematics nanopositioning stage," *Sensors Actuators A*, vol. 147, pp. 340-351, May 2008.

[3] W. Jung, D. T. McCormick, J. Zhang, L. Wang, N. C. Tien, and Z. Chen. "Three-dimensional endoscopic optical coherence tomography by use of a two-axis microelectromechanical scanning mirror," *Appl. Phys. Lett.*, vol. 88, pp. 163901, April 2006.

[4] D. T. McCormick, W. Jung, Y. C. Ahn, Z. Chen, and N. C. Tien. "A three dimensional real-time MEMS based optical biopsy system for in-vivo clinical imaging," in *Proc. Solid-State Sensors, Actuators and Microsystems Conf., 2007. TRANSDUCERS 2007*, pp. 203-208. IEEE, June 2007.

[5] A. D. Aguirre, P. R. Hertz, Y. Chen, J. G. Fujimoto, W. Piyawattanametha, L. Fan, and M. C. Wu. "Two-axis MEMS scanning catheter for ultrahigh resolution three-dimensional and en face imaging," *Opt. Express*, vol. 15, pp. 2445-2453, March 2007.

[6] K. Kumar, J. C. Condit, A. McElroy, N. J. Kemp, K. Hoshino, T. E. Milner, and X. Zhang. "Fast 3D in vivo swept-source optical coherence tomography using a two-axis MEMS scanning micromirror," *J. Optics A-Pure Appl. Opt.*, vol. 10, pp. 044013, April 2008.

[7] K. H. Jeong and L. P. Lee. "A novel microfabrication of a self-aligned vertical comb drive on a single SOI wafer for optical MEMS applications," *J. Micromech. Microeng.*, vol. 15, pp. 277, 2005.

[8] J. T. W. Yeow, V. X. D. Yang, A. Chahwan, M. L. Gordon, B. Qi, I. A. Vitkin, B. C. Wilson, and A. A. Goldenberg. "Micromachined 2-D scanner for 3-D optical coherence tomography," *Sensors Actuators A*, vol. 117, pp. 331-340, 2005.

[9] J. Singh, J. H. S. Teo, Y. Xu, C. S. Premachandran, N. Chen, R. Kotlanka, M. Olivo, and C. J. R. Sheppard, "A two axes scanning SOI MEMS micromirror for endoscopic bioimaging," *J. Micromech. Microeng.*, vol. 18, 2008.

[10] L. Liu, L. Wu, J. Sun, E. Lin, and H. Xie. "Miniature endoscopic optical coherence tomography probe employing a two-axis microelectromechanical scanning mirror with through silicon vias," *J. Biomed. Opt.*, vol. 16, pp. 026006, 2011.

[11] J. Sun, S. Guo, L. Wu, L. Liu, S. Choe, B. S. Sorg, and H. Xie. "3D in vivo optical coherence tomography based on a low-voltage, large-scan-range 2D MEMS mirror," *Opt. Express*, vol. 18, pp. 12065, May 2010.

[12] U. Izhar, A. B. Izhar, and S. Tatic-Lucic. "A multi-axis electrothermal micromirror for a miniaturized OCT system," *Sensors Actuators A*, vol. 167, pp. 152-161, 2011.

[13] K. H. Koh, T. Kobayashi, J. Xie, A. Yu, and C. Lee. "Novel piezoelectric actuation mechanism for a gimbal-less mirror in 2D raster scanning applications," *J. Micromech. Microeng.*, vol. 21, pp. 075001, 2011.

[14] Y. Zhu, W. Liu, K. Jia, W. Liao, and H. Xie. "A piezoelectric unimorph actuator based tip-tilt-piston micromirror with high fill factor and small tilt and lateral shift," *Sensors Actuators A*, vol. 167, pp. 495-501, March 2011.

[15] K. H. Kim, B. H. Park, G. N. Maguluri, T. W. Lee, F. J. Rogomentich, M. G. Bancu, B. E. Bouma, J. F. de Boer, and J. J. Bernstein. "Two-axis magnetically-driven MEMS scanning catheter for endoscopic high-speed optical coherence tomography," *Opt. Express*, vol. 15, pp. 18130-18140, December 2007.

[16] Y. Q. Fu, M. Hu, H. Du, J. Luo, A. J. Flewitt, and W. I. Milne. "Micromirror structure based on TiNi shape memory thin films," in *Proc. Smart Materials, Nano-, and Micro-Smart Systems*, pp. 145-153, August 2005.

[17] E.Pengwang, K. Rabenorosoa, M. Rakotondrabe and N. Andreff, "A hybrid electrostatic-piezoelectric integrative actuated microsystem for robot-assisted laser phonomicrosurgery", RGC (Russian Bavarian Conference on Bio-Medical Engineering), Hannover Germany, October 2013.